Catalysis Letters 24 (1994) 23–30

The characterization of carbonaceous species from CO hydrogenation on single crystal Ru(0001) and Ru(11$\bar{2}$0) catalysts with high-resolution electron energy-loss spectroscopy

Ming-Cheng Wu, D. Wayne Goodman [1]

Department of Chemistry, Texas A&M University, College Station, TX 77843-3255, USA

and

Gerry W. Zajac

Amoco Research Center, Amoco Corporation, PO Box 3011, MC B-5, Naperville, IL 60566-7011, USA

Received 2 July 1993; accepted 15 October 1993

The CO hydrogenation on single-crystal ruthenium catalysts has been studied utilizing an elevated-pressure micro-reactor and high resolution electron energy loss spectroscopy (HREELS). It is found that carbonaceous deposits identified following CO hydrogenation are essentially identical to those observed in the study of methane decomposition. Three distinct forms of carbonaceous intermediates are identified; these are methylidyne (CH), vinylidene (CCH_2), and graphitic carbonaceous species.

Keywords: CO hydrogenation; single crystal Ru catalysts; carbonaceous species; surface science studies

1. Introduction

The characterization of carbonaceous deposits on supported transition metal catalysts from synthesis gas has received much attention in catalytic research. This issue is critical to the understanding of mechanisms of various reactions, such as CO methanation and Fischer–Tropsch synthesis.

With the use of transient response tracing technique and ^{13}C nuclear magnetic resonance spectroscopy (NMR), Bell and co-workers [1–3] have shown that three

---

[1] To whom correspondence should be addressed.

forms of carbonaceous residues, designated as C_α, C_β and C_γ, are present on silica supported Ru catalysts during CO hydrogenation. The C_α species reacts rapidly with hydrogen and appears to be the principal form of carbon for the formation of hydrocarbons from synthesis gas. A less reactive surface species (C_β) actually contains two distinct components, designated as $C_{\beta1}$ and $C_{\beta2}$. The NMR spectra of the $C_{\beta1}$ and $C_{\beta2}$ species are consistent with those of linear alkyl species [3]. Finally, the C_γ species is least active and corresponds to graphitic carbon.

Electron spectroscopy [4–8] and in situ infrared spectroscopy [9–11] have also been utilized to identify carbonaceous residues on various transition metal catalysts during CO hydrogenation. Using Auger electron spectroscopy (AES) and X-ray photoelectron spectroscopy (XPS), Bonzel and Krebs [8] could distinguish three forms of carbonaceous intermediates after CO hydrogenation on Fe(110); these are a CH_x species, a carbidic carbon phase, and a graphite phase. The CH_x and the carbidic carbon phases were active towards hydrogenation, whereas the graphitic carbon was inactive under the chosen experimental conditions. In situ infrared spectroscopic studies [9], on the other hand, revealed that in addition to CO bands, some oxygenated species, such as surface formate species, were present on alumina supported Ru catalysts after CO hydrogenation. These latter species were found to reside on the support and considered to be spectators [9]. At higher temperatures, a deactivation of the catalysts is associated with a decrease in intensity of the CO band and a buildup of a passive form of carbon.

Despite these previous efforts to identify carbonaceous intermediates formed during CO hydrogenation, the chemical composition of the active form of carbon remains controversial. Nevertheless, on the basis of previous spectroscopic studies, the following conclusions can be drawn: (1) carbidic carbon, which may consist of a range of hydrocarbon intermediates including the single carbon adatom, is likely to be an intermediate in Fischer–Tropsch synthesis; (2) graphitic carbon acts as a poison.

The present study stems from our recent investigations of carbonaceous species on single crystal Ru catalysts from methane decomposition [12]. High-resolution electron energy-loss spectroscopy (HREELS) has been utilized to identify various forms of hydrocarbonaceous intermediates following methane decomposition. It was found [12] that three distinct forms of carbonaceous species exist on both Ru(0001) and Ru($11\bar{2}0$) surfaces; these are methylidyne (CH), vinylidene (CCH_2) and graphitic carbonaceous species. A fourth species, ethylidyne, exists only on Ru($11\bar{2}0$) for the methane decomposition temperature at $T \leqslant 400$ K. Our combined elevated pressure measurements/HREELS studies [12] further showed that the vinylidene species is likely to be the key intermediate to ethane. In the present study, the chemical nature of the carbonaceous residues on Ru catalysts during CO hydrogenation are characterized and the surface species compared with the carbon types found following methane decomposition.

2. Experimental

The studies were carried out in a combined elevated-pressure reactor / ultrahigh vacuum (UHV) system, described elsewhere [12], equipped with HREELS, Auger electron spectroscopy (AES), low energy electron diffraction (LEED) and temperature programmed desorption (TPD), and for sample heating and cooling. After completion of surface cleaning in the surface analytical chamber, the single-crystal Ru catalyst could be transferred in situ into the reaction chamber through a double-stage differentially pumped teflon sliding seal. The details of crystal cleaning and handling can be found elsewhere [12].

Carbon monoxide and hydrogen gases were purchased from Matheson at a nominal purity of 99.99% and 99.9995%, respectively. CO was purified with a cryogenic method in which the gas-containing glass bulb was immersed in a liquid nitrogen Dewar for a 12 h period. This method has been found to be extremely effective in removing impurity gases, particularly metal carbonyls [13]. Hydrogen gas was purified in a similar manner. Two gases with a desired composition then were fully mixed before admission into the reaction chamber.

The following procedure was used in carrying out a reaction: (1) the fully mixed gas was introduced into the reactor with the clean crystal at room temperature; (2) the crystal temperature was quickly raised to a reaction temperature where it was held for the length of time of that particular reaction; (3) heating was turned off simultaneously while exhausting the gas; (4) the crystal was transferred to the HREELS position of the surface analytical chamber.

HREELS data then were collected following the above procedure. The spectra were acquired using an electron beam with a primary energy of $E_p \approx 2$–4 eV and at an incident angle of the electron beam of 60° about the surface normal. The other parameters used in obtaining the EELS spectra presented here were the following: spectral resolution (full width at half maximum of the elastically reflected electron beam), 50–70 cm^{-1}; typical count rate in the elastic peak from the clean surface, 500000 Hz.

3. Results and discussion

CO hydrogenation on the Ru(0001) and Ru(11$\bar{2}$0) surfaces was carried out in the reaction chamber in 8.5 Torr of reactants with a CO : H_2 ratio of 1 : 4 and subsequently examined in the surface analytical chamber using HREELS. Displayed in fig. 1a is a HREELS spectrum acquired following CO hydrogenation on a Ru(0001) surface at $T = 600$ K. Exposing the surface to the reactants gives rise to several distinct loss features in the 200–4000 cm^{-1} frequency range of the HREELS spectra. The losses at 450, 1760 and 1985 cm^{-1} are due to adsorbed reactants, while the features at 815, 1400 and 2990 cm^{-1} arise from hydrocarbonaceous species due to CO hydrogenation. Heating the sample momentarily to 500 K in the UHV

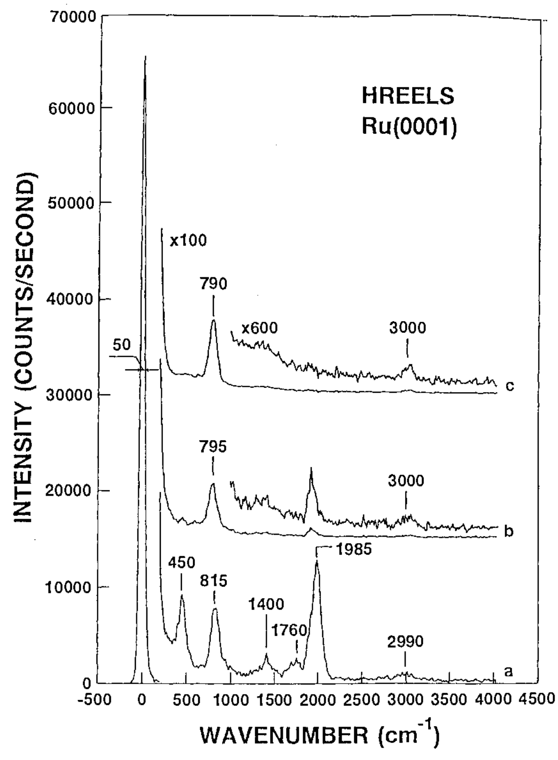

Fig. 1. HREELS spectra acquired following CO hydrogenation on a Ru(0001) surface. The spectra were obtained (a) immediately after reaction and (b) after momentarily heating to 500 K in ultra-high vacuum. The reaction conditions used were: $P = 8.5$ Torr with $P_{CO}/P_{H_2} = 1/4, T = 600$ K, $t = 5$ min. Spectrum c was obtained following methane decomposition on Ru(0001). The methane decomposition was carried out with the following reaction parameters: $P_{CH_4} = 5$ Torr, $t_{CH_4} = 2$ min, $T_{CH_4} = 600$ K. All spectra were collected at $E_p \approx 4.1$ eV and at the specularly reflected beam direction.

chamber removes a major portion of the adsorbed CO and eliminates the loss feature at 1400 cm^{-1}, as shown in fig. 1b. The origin of the loss at 1400 cm^{-1} is not known; however, this feature likely arises from a hydrocarbonaceous species containing CH_2 groups since the 1400 cm^{-1} loss corresponds to the scissoring mode of CH_2. A very weak feature is apparent between 1100 and 1500 cm^{-1} in spectra b and c of fig. 1.

It is noteworthy that spectrum b in fig. 1 exhibits features essentially identical to those of spectrum c which was obtained following methane decomposition on a Ru(0001) surface. This result clearly demonstrates that the hydrocarbonaceous types found in CO hydrogenation are the same as those observed in methane decomposition.

The loss features in spectra b and c exhibit a distinct loss intensity pattern, i.e. an intense loss at ~ 800 cm^{-1} and a weak feature at ~ 3000 cm^{-1}. By analogy to the results obtained from other HREELS studies [14–20] and those of organometallic compounds [21,22], the losses near 800 and 3000 cm^{-1} can be attributed to the CH bending mode (δ(CH)) and the CH stretching mode (ν(CH)), respectively, of a methylidyne species (CH). The great similarity in relative mode intensities between these results and those of previous studies [14–20] further supports the assignments of these losses.

CO hydrogenation has also been carried out at several reaction temperatures on Ru(0001). It was found that in addition to the loss features arising from the methylidyne species, two weaker loss peaks at 1160 and 1395 cm^{-1} were evident at temperatures between 500 and 550 K in HREELS spectra (not shown here). These two weak features were also observed in methane decomposition and attributed to the carbon–carbon stretch (ν(C=C)) and the CH_2 scissors ($\delta(CH_2)$), respectively, of a vinylidene intermediate [12]. The detailed assignment of the loss features and the identification of the corresponding surface species can be found elsewhere [12].

Finally, it is noteworthy there is a barely perceptible broad feature between 100 and 1500 cm^{-1} in spectra b and c of fig. 1. This weak feature, observed only at temperatures exceeding 600 K, likely arises from the ring breathing mode of surface graphite [23]. The details of HREELS studies of graphitic carbon on Ru surfaces including those utilizing scanning tunnelling microscopy (STM) are described elsewhere [24].

The CO hydrogenation on the Ru(11$\bar{2}$0) surfaces has also been carried out in 8.5 Torr of reactants with a CO : H_2 ratio of 1 : 4 and subsequently examined in the surface analytical chamber using HREELS. Fig. 2a shows a HREELS spectrum acquired following CO hydrogenation on Ru(11$\bar{2}$0) at $T = 600$ K. Similar to CO hydrogenation on Ru(0001), the losses at 470, 1800 and 1980 cm^{-1} are due to adsorbed CO from the reactants. The remaining loss features in spectrum a are essentially identical to those in spectrum b obtained following methane decomposition on a Ru(11$\bar{2}$0) surface. CO hydrogenation has also been carried out at several reaction temperatures. It was found that the loss features arising from hydrocarbonaceous species in the HREELS spectra (not shown here) were the same as those observed in methane decomposition. The above results clearly indicate the formation of similar types of hydrocarbonaceous intermediates on Ru(11$\bar{2}$0) following CO hydrogenation as those observed in methane decomposition. By analogy to the results of methane decomposition [12], the losses at 845 and 3005 cm^{-1} can be attributed to the CH bending mode (δ(CH)) and the CH stretching mode (ν(CH)), respectively, of a methylidyne species (CH). Likewise, the losses at 1120, 1380, 1590 and 3005 cm^{-1} are attributed to the CH_2 rock ($\rho(CH_2)$), the CH_2 scissors ($\delta(CH_2)$), the carbon–carbon stretch (ν(C=C)) and the CH_2 stretch ($\nu(CH_2)$), respectively, of a vinylidene intermediate (CCH_2). The detailed assignment of these losses and the identification of the corresponding surface species can be found elsewhere [12].

In summary, the above HREELS studies reveal that three distinct forms of sur-

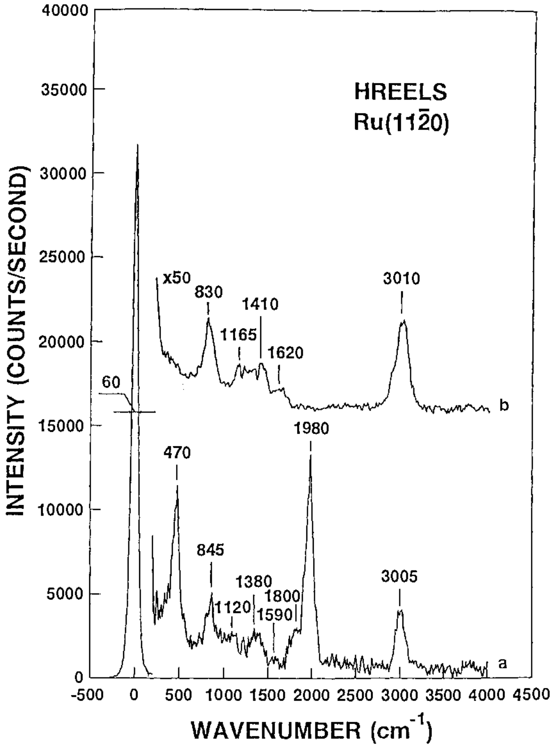

Fig. 2. HREELS spectra acquired following CO hydrogenation on a Ru(11$\bar{2}$0) surface. Spectrum a was obtained with the same reaction conditions as those in fig. 1. Spectrum b was obtained following methane decomposition on Ru(11$\bar{2}$0). The methane decomposition was carried out with the following reaction parameters: $P_{CH_4} = 5$ Torr, $t_{CH_4} = 2$ min, $T_{CH_4} = 600$ K. All spectra were collected at $E_p \approx 2.2$ eV and at the specularly reflected beam direction.

face carbonaceous species, identified as methylidyne, vinylidene and graphitic carbonaceous species, exist on both the Ru(0001) and Ru(11$\bar{2}$0) surfaces following CO hydrogenation. The carbon types found in CO hydrogenation under the experimental conditions employed are the same as those observed in methane decomposition on the Ru surfaces. No oxygenated surface species, except CO, is observed following CO hydrogenation on the Ru surfaces.

In the preceding sections, we have attributed the loss features at ~ 460, ~ 1780 and ~ 1980 cm^{-1} to adsorbed CO. Fig. 3 shows HREELS spectra acquired following the reaction of CO with the Ru(0001) and Ru(11$\bar{2}$0) surfaces. The reactions were carried out at 500 K with 5 Torr of CO for 2 min. Exposing the Ru surfaces to CO gives rise to only two loss peaks at 445 and 2040 cm^{-1} for Ru(0001) (fig. 3a), and at 460 and 2060 cm^{-1} for Ru(11$\bar{2}$0) (fig. 3b). These two losses can be attributed to the carbon–metal stretch and the carbon–oxygen stretch, respectively, of adsorbed CO. Therefore, the observation of the CO stretch at the lower frequency (~ 1780 cm^{-1}) in the presence of hydrogen during reaction is a clear indication for

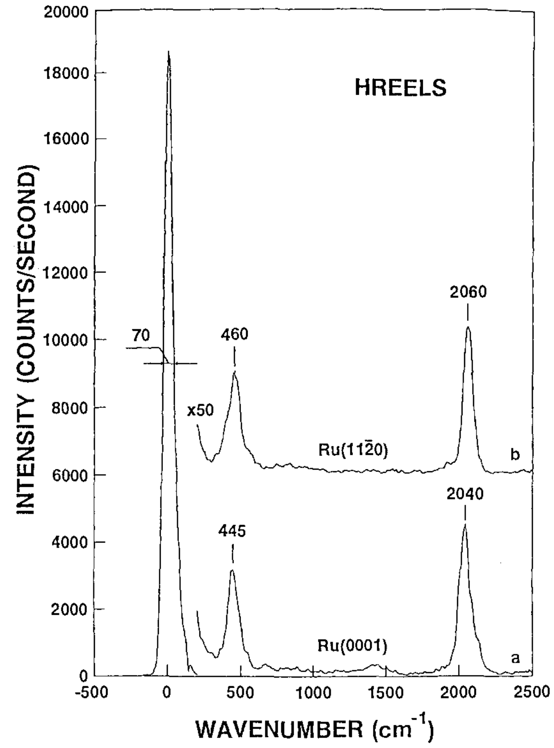

Fig. 3. HREELS spectra acquired following the reaction of CO with (a) the Ru(0001) surface and (b) the Ru(11$\bar{2}$0) surface. The reactions were carried out at 500 K with 5 Torr of CO for 2 min.

the weakening of CO bonds. The CO bond softening has been previously observed in the studies of co-adsorption with hydrocarbons [25]. A possible mechanism for the CO bond weakening has been suggested to consist of donation of electrons from the hydrocarbon to the metal and backdonation into the antibonding π^* orbital of the CO molecule [25]. In the present study, it is proposed that CO in this adsorption state is likely to be a precursor to the dissociated state which may be responsible for the formation of the hydrocarbonaceous residues.

4. Conclusions

HREELS spectroscopy has been used to characterize various forms of adsorbed hydrocarbon intermediates present on single-crystal Ru catalysts following CO hydrogenation. The carbon types identified in this study were essentially identical to those observed in the study of methane decomposition on the Ru catalysts under the experimental conditions employed. Three distinct forms of surface species on Ru(0001) and Ru(11$\bar{2}$0) were identified these are methylidyne (CH), vinylidene

(CCH_2), and graphitic carbonaceous species. The presence of a CO species with a soft CO bond after the CO hydrogenation reaction was observed. CO in this adsorption state is likely to be a precursor to the dissociated state.

Acknowledgement

We acknowledge the support of this work by the Gas Research Institute and Alternative Feedstock Development Division of Amoco Corporation.

References

[1] P. Winslow and A.T. Bell, J. Catal. 86 (1984) 158.
[2] T.M. Duncan, P. Winslow and A.T. Bell, J. Catal. 93 (1985) 1.
[3] T.M. Duncan, J.A. Reimer, P. Winslow and A.T. Bell, J. Catal. 95 (1985) 305.
[4] L. Papagno, L.S. Caputi, F. Ciccacci and C. Mariani, Surf. Sci. 128 (1983) L209.
[5] F.J. Himpsel, K. Christmann, P. Heimann, D.E. Eastman and P.J. Feibelman, Surf. Sci. 115 (1982) L159.
[6] D.W. Goodman, R.D. Kelley, T.E. Madey and J.M. White, J. Catal. 64 (1980) 479.
[7] D.W. Goodman and J.M. White, Surf. Sci. 90 (1979) 201.
[8] H.P. Bonzel and H.J. Krebs, Surf. Sci. 91 (1980) 499.
[9] R.A. Dalla Betta and M. Shelef, J. Catal. 48 (1977) 111.
[10] J.G. Ekerdt and A.T. Bell, J. Catal. 58 (1979) 170.
[11] F. Solymosi, I. Tombacz and M. Kocsis, J. Catal. 75 (1982) 78.
[12] M.-C. Wu and D.W. Goodman, J. Am. Chem. Soc., submitted.
[13] W.K. Kuhn, J. Szanyi and D.W. Goodman, Surf. Sci. 274 (1992) L611.
[14] J.E. Parmeter, M.M. Hills and W.H. Weinberg, J. Am. Chem. Soc. 108 (1986) 3563.
[15] M.M. Hills, J.E. Parmeter, C.B. Millins and W.H. Weinberg, J. Am. Chem. Soc. 108 (1986) 3554.
[16] P. Jakob, A. Cassuto and D. Menzel, Surf. Sci. 187 (1987) 407.
[17] H. Steiniger, H. Ibach and S. Lehwald, Surf. Sci. 117 (1982) 685.
[18] S. Lehwald and H. Ibach, Surf. Sci. 89 (1979) 425.
[19] L.H. Dubois and G.A. Somorjai, Am. Chem. Soc. Symp. Ser. 32 (1980) 1.
[20] J.A. Gates and L.L. Kesmodel, Surf. Sci. 124 (1983) 68.
[21] M.W. Howard, S.F. Kettle, I.A. Oxton, D.B. Powell, N. Sheppard and P. Skinner, J. Chem. Soc. Faraday Trans. II 77 (1981) 397.
[22] I.A. Oxton, Spectrochim. Acta A 38 (1982) 181.
[23] T. Aizawa, R. Souda, Y. Ishizawa, H. Hirano, T. Yamada and K.-I. Tanaka, Surf. Sci. 237 (1990) 194.
[24] M.-C. Wu, Q. Xu and D.W. Goodman, in preparation.
[25] H. Ibach and G.A. Somorjai, Appl. Surf. Sci. 3 (1979) 293.